Hydrogen Balmer Series Measurements in Laser-Induced Air Plasma

L D Swafford, D M Surmick, M J Witte, A C Woods, G Gautam, and C G Parigger

University of Tennessee Space Institute, 411 B.H. Goethert Parkway, Tullahoma, TN 37388, USA

E-mail: cparigge@tennessee.edu

Abstract. Time-resolved spectroscopy is employed to analyze micro plasma generated in laboratory air. Stark-broadened emission profiles for hydrogen alpha and beta allow us to determine plasma characteristics for specific time delays after plasma generation. Stark shift, asymmetry, and full width half maximum measurements are used to infer electron density. The measurements of hydrogen alpha and beta Balmer series line shapes are analyzed using various theory results. Our laser-induced breakdown spectroscopy arrangement uses a Q-switched Nd:YAG laser operating at the fundamental wavelength of 1064 nm that is focused for plasma generation. The hydrogen alpha and beta lines emerge from the free electron background radiation for time delays larger than 0.3 μs and 1.4 μs, respectively. Neutral and ionized nitrogen emission lines allow us to infer electron density for time delays from 0.1 to 10 μs. The electron density values are compared with results obtained from hydrogen Balmer series line shapes.

1. Introduction

Laser-Induced Breakdown Spectroscopy (LIBS) techniques are employed to measure micro-plasma emissions in laboratory air. Figure 1 illustrates the schematic experimental arrangement.

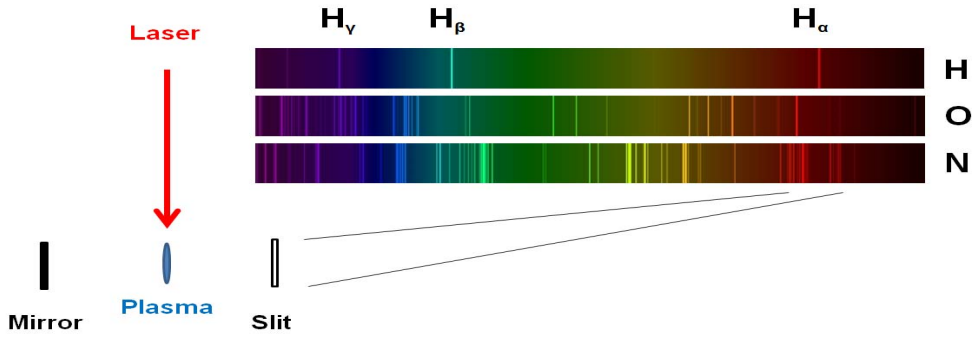


Figure 1. Schematic experimental arrangement. The laser-induced plasma is generated by focusing pulsed radiation at 1064 nm from the top. Lenses, a Czerny-Turner spectrometer and an intensified array detector (not shown) are used to collect, disperse and record spectra.

Content from this work may be used under the terms of the Creative Commons Attribution 3.0 licence. Any further distribution of this work must maintain attribution to the author(s) and the title of the work, journal citation and DOI.
Published under licence by IOP Publishing Ltd

Figure 1 also shows discharge spectra for hydrogen, oxygen, and nitrogen, and the wavelength ranges of interest for measurements of H_α near 656.28 nm and H_β near 486.14 nm. Time-resolved spectral data records are obtained by use of an Intensified Linear Diode Array (Intensified LDA, model 1460 EG&G Princeton) and/or an Intensified Charge Coupled Device (ICCD, Andor model iSTAR 334T) connected to a 0.64 m Czerny-Turner Spectrometer (model Jobin Yvon 640) [1, 2, 3]. For the images reported in this work, the micro-plasma is generated parallel to the spectrometer slit by focusing Nd:YAG fundamental laser radiation at 1064 nm from the top using f# = 4 optics. Emissions from the plasma are imaged close to 1:1 onto the spectrometer slit, and in addition, we utilize a flat mirror to explore effects of self absorption. Self-absorption investigations are based on comparing results with and without the flat mirror [4, 5, 6] and by determining electron density from nitrogen lines [7].

2. Results

The emission spectra are recorded by averaging 81 consecutive plasma generation events, with the ICCD detector set to record 276 spectra spatially-resolved along the slit height. Figure 2 illustrates typical results. The images are wavelength calibrated, detector dark-count subtracted, and detector-sensitivity corrected.

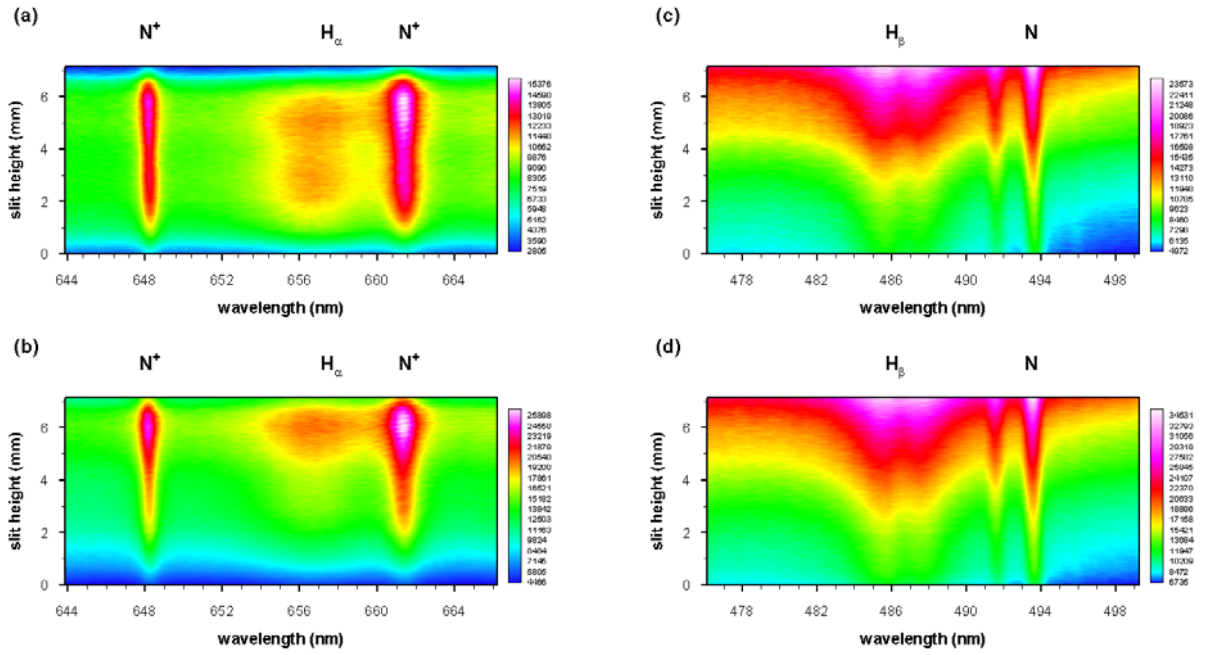


Figure 2. Recorded spectra vs. slit height. H_α (a) without mirror, (b) with mirror; $\Delta\tau = 0.3$ μs. H_β (c) without mirror, (d) with mirror; $\Delta\tau = 3.0$ μs.

A mirror and an additional lens was used to retro-reflect emissions through the laser-induced plasma. A gate-width of 10 ns was employed. For this experiment, we combined as well 2 vertical camera pixels for an effective pixel size of 26 μm $\times$ 26 μm. Early in the plasma decay, for delays of 0.3 μs, expansion speeds are typically hypersonic (or larger than Mach 5) yet for 3.0 μs time delays, speeds are supersonic. For an expansion speed of Mach 5, using a 10 ns gate width and an effective time delay of 2 ns by introducing the mirror, one finds on the order of 20 μm spatial displacement due to plasma evolution yet this is for 1:1 imaging smaller than the 26 μm linear dimension of two vertically combined pixels.

The electron number densities for the hydrogen alpha and beta line was determined from the measured the full-width half maximum (FWHM) of the atomic emission spectra at a given time delay, using Equation (1) below [8]:

$$\mathrm{H}_\alpha:\ N_{e,\alpha}[m^{-3}] = (w_\alpha[nm]/1.098)^{1.47135}\times 10^{23}; \qquad \mathrm{H}_\beta:\ N_{e,\beta}[m^{-3}] = (w_\beta[nm]/4.8)^{1.46808}\times 10^{23}. \tag{1}$$

The FWHM measurement is facilitated by fitting of measured spectra. For hydrogen beta fitting, contributions from Lorentzian and Gaussian components of spectral broadening are included. The shape of the Stark broadened line varies with N_e which also corresponds with changes of the asymmetry. Measurement of the Stark profile FWHM is reasonable approach to determine N_e. For our purposes, we use the FWHM of the fitted Voigt profile, and use empirical formulae [8], tabulated profiles [9] or results from convergent theory [10, 11].

In addition, we evaluated use of the asymmetric line shapes for the purpose of determining electron density using Equ (2) [12]:

$$\mathrm{H}_\beta:\ N_{e,\beta}[10^{23}\ m^{-3}] = 0.14(\rho[\%])^3; \qquad \rho = 2(I_B - I_R)/(I_B + I_R), \tag{2}$$

where the blue I_B, and red, I_R, intensity values denote the lower and higher wavelength peaks of the Stark-broadened hydrogen beta profile. Details of this study are elaborated in Ref. [12] and show that for hydrogen beta lines, the accuracy of N_e determination is much improved when using the FWHM approach.

In the analysis of recorded H_α spectra, ionized nitrogen lines at 648.2 nm and 661.1 nm can be used as well [7] to determine electron density. These two lines can be seen in Figures 2 (a) and (b) at the low and high wavelength side of the 656.28 nm hydrogen Balmer Series line. In turn, for the H_β line, the neutral nitrogen line at 493.51 nm can be used, see Figs. 2 (c) and (d). Inferred electron densities for a delay of $\Delta\tau = 0.3$ μs from optical breakdown (from only H_α profiles) amount to 14 to 20 $\times$ 10^{23} m^{-3}. Yet N^+ diagnostics [7] indicate electron densities of $\simeq 12 \times 10^{23}$ m^{-3}. Consequently, self-absorption is evident for the 0.3 μs data set. For a time delay $\Delta\tau$ of 0.4 μs, hardly any self-absorption occurs; for time delays of 3.0 μs self-absorption effects appear to be insignificant as well. For the 3.0 μs data sets, the inferred electron densities from hydrogen alpha and hydrogen beta agree within experimental error, and amount to 1.1 $\times$ 10^{23} m^{-3} and 0.96 $\times$ 10^{23} m^{-3}, respectively.

3. Conclusions

Determination of the electron density from the FWHM of the Balmer H_α and H_β line proves to be more accurate than from asymmetry of the line shapes. Difficulty of determining the asymmetry parameters for especially incomplete profiles increases the uncertainty. For larger electron densities, or for shorter time delays from optical breakdown, the uncertainties become too large for determining N_e from the asymmetry parameter. The electron density FWHM diagnostic shows the effects of hydrogen alpha self-absorption for the very early time delays of 0.3 μs, or when hydrogen alpha emerges from the free electron background. Hydrogen alpha and hydrogen beta measurement results of electron density agree for time delays of 3.0 μs within experimental error margins, and appear to only show insignificant effects due to self-absorption. The studies reported here focus on optically generated plasma in laboratory air; however, it is expected that self-absorption effects are more readily observable during laser ablation processes due to significantly higher electron density for laser-radiation interacting with solids.

Acknowledgments

The authors thank for support of this work by the Center for Laser Applications at the University of Tennessee Space Institute, and we gratefully acknowledge discussions with Dr. Eugene Oks on Stark-broadened line shapes.

References

[1] Parigger C G 2010 *Int. Rev. At. Mol. Phys.* **1** 129
[2] Parigger C G 2013 *Spectrochim. Acta Part B* **79-80** 4
[3] Parigger C G, Woods A C, Witte M J, Swafford L D, Surmick D M 2014 *JoVE* **84** E51250
[4] Moon H, Herrera K K, Omenetto N, Smith B W, Winefordner J D 2009 *Spectrochim. Acta Part B* **64**, 702
[5] Konjević N 1999 *Phys. Rep.* **316** 339
[6] El Sherbini A M, El Sherbini Th M, Hegazy H, Cristoforetti G, Legnaoili S, Palleschi V, Pardini L, Salvetti A, Tognoni E. 2005 *Spectrochim. Acta Part B* **60** 1573
[7] Konjević N, Lesage A, Fuhr J R, Wiese W L 2002 *J. Phys. Chem. Ref. Data* **31** 819
[8] Konjević N, Ivković M, Sakan N 2012 *Spectrochim. Acta Part B* **76** 593
[9] Griem HR 1964 *Plasma Spectroscopy*, McGraw-Hill, New York, 1964
[10] Oks E 2006 18$^{\text{th}}$ ICSLS: AIP Conf. Proceedings **874** 19
[11] Parigger C G, Plemmons D H, Oks E 2003 *Appl. Opt.* **42** 5992
[12] Parigger C G, Swafford L D, Woods A C , Surmick D M, Witte M J 2014 *Spectrochim. Acta Part B* **99** 28